The effective permeability of a random medium

1987 J. Phys. A: Math. Gen. 20 4661

(http://iopscience.iop.org/0305-4470/20/14/012)

J. Phys. A: Math. Gen. **20** (1987) 4661-4672. Printed in the UK

The effective permeability of a random medium

I T Drummond and R R Horgan

Department of Applied Mathematics and Theoretical Physics, University of Cambridge, Silver Street, Cambridge CB3 9EW, UK

Received 12 February 1987

Abstract. We investigate the effective permeability of a heterogeneous random medium by numerical simulation and by self-consistent perturbation theory for a class of models including the log-normal model. For a reasonable range of parameters we find close agreement between the simulation and the perturbative calculation. This suggests that both methods may be useful for appropriate models. However the simulation approach is widely applicable in circumstances where a perturbation calculation is not possible.

1. Introduction

There are many situations in which it is useful to be able to predict the large-scale behaviour of a fluid flowing through a region of variable permeability (Dullien 1979, Scheidegger 1974). Recently King (1985) has shown how the effective permeability of a random medium may be calculated by means of a perturbation series in the fluctuating part of the local permeability.

In this paper we extend these calculations to higher order, for a class of models of random media of which the log-normal model is an example. We show how to reformulate the perturbation series in a self-consistent manner and present a comparison of these theoretical results with those of a numerical simulation.

A brief discussion of flow through a medium of variable permeability and an associated diffusion problem is presented in § 2. In § 3 we discuss the class of models we are able to deal with theoretically, and indicate briefly their applicability. The perturbation series for the effective permeability is formulated in § 4 and evaluated up to terms of fourth order. In § 5 we introduce certain resummation techniques to simplify the series and we also reformulate it in a self-consistent manner. The numerical simulation is described in § 6 and numerical comparisons are studied in § 7.

2. Flow through a randomly porous medium

The steady flow of a fluid through a medium with a permeability distribution $\kappa(\boldsymbol{x})$ satisfies Darcy's law (Dullien 1979, Scheidegger 1974), namely

$$\boldsymbol{u}(\boldsymbol{x}) = -\kappa(\boldsymbol{x})\nabla p(\boldsymbol{x}) \tag{2.1}$$

where $\boldsymbol{u}(\boldsymbol{x})$ is the velocity and $p(\boldsymbol{x})$ is the pressure distribution in the fluid. For an incompressible fluid the pressure satisfies

$$\nabla \cdot (\kappa(\boldsymbol{x})\nabla p) = 0. \tag{2.2}$$

0305-4470/87/184661+12$02.50

If a unit point source of fluid is present within the medium at $\boldsymbol{x}'$ then (2.2) is altered to

$$\nabla \cdot (\kappa(\boldsymbol{x})\nabla p) = -\delta(\boldsymbol{x}-\boldsymbol{x}'). \tag{2.3}$$

We are then interested in that solution of (2.3), namely

$$p = G(\boldsymbol{x}, \boldsymbol{x}') \tag{2.4}$$

which satisfies *homogeneous* boundary conditions appropriate to the geometrical layout of the particular problem under consideration.

For the purposes of numerical simulation it is useful to consider also the diffusion problem associated with (2.2), namely

$$\nabla \cdot (\kappa(\boldsymbol{x})\nabla p) = \partial p/\partial \tau \tag{2.5}$$

where, it should be emphasised, τ is an artificial time, distinct from real time, so far as the permeability problem is concerned. Of course (2.5) is independently interesting.

Any solution of (2.5) which satisfies the physical boundary conditions of the original problem will relax to the correct solution of (2.2) as $\tau \to \infty$. Furthermore if $F(\boldsymbol{x}, \boldsymbol{x}', \tau)$ is that solution of (2.5) satisfying *homogeneous* boundary conditions together with the requirement

$$F(\boldsymbol{x}, \boldsymbol{x}', 0) = \delta(\boldsymbol{x}-\boldsymbol{x}') \tag{2.6}$$

then

$$G(\boldsymbol{x}, \boldsymbol{x}') = \int_0^\infty \mathrm{d}\tau\, F(\boldsymbol{x}, \boldsymbol{x}', \tau). \tag{2.7}$$

This emphasises the close connection between the two problems.

The aim of our calculation is to predict the mean or effective pressure distribution in a given fluid flow, from a knowledge of the statistical properties of the permeability $\kappa(\boldsymbol{x})$. Details of particular models will be enlarged on later; however, for reasons of simplicity we will always assume large-scale homogeneity and isotropy of the medium. It is sufficient therefore to consider the Green function problem (2.3) for an infinite medium with vanishing boundary conditions at infinity. The statistical properties of the medium are incorporated by computing an effective Green function $\mathscr{G}(\boldsymbol{x}-\boldsymbol{x}')$ as the ensemble average of $G(\boldsymbol{x}, \boldsymbol{x}')$. Thus

$$\mathscr{G}(\boldsymbol{x}-\boldsymbol{x}') = \langle G(\boldsymbol{x}, \boldsymbol{x}') \rangle \tag{2.8}$$

where $\langle A \rangle$ denotes the average of A over the ensemble from which $\kappa(\boldsymbol{x})$ is drawn.

At large distances we expect

$$\mathscr{G}(\boldsymbol{x}-\boldsymbol{x}') = \frac{1}{4\pi\kappa_e|\boldsymbol{x}-\boldsymbol{x}'|} \tag{2.9}$$

where κ_e is the effective permeability of the medium. It is κ_e which determines the large-scale behaviour of the mean pressure distribution.

If we define the Fourier transform of $\mathscr{G}(\boldsymbol{x}-\boldsymbol{x}')$ thus:

$$\bar{\mathscr{G}}(\boldsymbol{k}) = \int \mathrm{d}^3\boldsymbol{x} \exp[-\mathrm{i}\boldsymbol{k}\cdot(\boldsymbol{x}-\boldsymbol{x}')]\mathscr{G}(\boldsymbol{x}-\boldsymbol{x}') \tag{2.10}$$

then (2.9) implies that, for $\boldsymbol{k} \to 0$,

$$\bar{\mathscr{G}}(\boldsymbol{k}) = \frac{1}{\kappa_e \boldsymbol{k}^2}. \tag{2.11}$$

Of course

$$\mathscr{G}(\boldsymbol{x}-\boldsymbol{x}') = \int_0^\infty \mathrm{d}\tau\, \mathscr{F}(\boldsymbol{x}-\boldsymbol{x}', \tau) \tag{2.12}$$

where

$$\mathscr{F}(\boldsymbol{x}-\boldsymbol{x}', \tau) = \langle F(\boldsymbol{x}, \boldsymbol{x}', \tau)\rangle. \tag{2.13}$$

As $\tau \to \infty$

$$\mathscr{F}(\boldsymbol{x}-\boldsymbol{x}', \tau) = \frac{1}{(4\pi\kappa_e\tau)^{3/2}} \exp\left(-\frac{(\boldsymbol{x}-\boldsymbol{x}')^2}{4\kappa_e\tau}\right) \tag{2.14}$$

so that κ_e also controls the dispersion at large 'times' τ in the diffusion version of the problem. This is the property we will use to obtain κ_e by numerical simulation of the diffusion process.

3. Types of model

The models of random media investigated in this paper are specified by a permeability distribution of the form

$$\kappa(\boldsymbol{x}) = f(\phi(\boldsymbol{x})) \tag{3.1}$$

where

$$f(\phi) = \sum_{n=0}^{\infty} \frac{c_n}{n!}(\lambda\phi)^n \tag{3.2}$$

and $\phi(\boldsymbol{x})$ is a Gaussian random variable with zero mean and a two-point correlation function

$$\Delta(\boldsymbol{x}-\boldsymbol{x}') = \langle\phi(\boldsymbol{x})\phi(\boldsymbol{x}')\rangle \tag{3.3}$$

normalised so that $\Delta(0) = 1$. The choice $c_n = \kappa_0$ for all n yields the log-normal model:

$$\kappa(\boldsymbol{x}) = \kappa_0 \exp(\lambda\phi(\boldsymbol{x})). \tag{3.4}$$

The models are further specified by giving the form of $\Delta(\boldsymbol{x}-\boldsymbol{x}')$, which it is natural to do in terms of its Fourier transform:

$$\bar{\Delta}(\boldsymbol{k}) = \int \mathrm{d}^3\boldsymbol{k} \exp[-\mathrm{i}\boldsymbol{k}\cdot(\boldsymbol{x}-\boldsymbol{x}')]\Delta(\boldsymbol{x}-\boldsymbol{x}'). \tag{3.5}$$

Particular choices of $\bar{\Delta}(\boldsymbol{k})$ will be studied later.

It is worth noting that the mean permeability is

$$\kappa_m = \langle\kappa(\boldsymbol{x})\rangle = \sum_{n=0}^{\infty} \frac{c_{2n}}{n!}\left(\frac{\lambda^2}{2}\right)^n \tag{3.6}$$

which in the log-normal model becomes

$$\kappa_m = \exp(\tfrac{1}{2}\lambda^2). \tag{3.7}$$

The justification for considering models of this type is partly the ease with which they can be analysed both theoretically and by numerical simulation. However they

are not trivial and can be used to represent a variety of types of medium. The log-normal model, for example, yields a smooth distribution of permeability about the mean value, while avoiding the unphysical situation of negative permeability.

Other choices, such as

$$f(\phi) = \kappa_0(1 + \alpha \tanh \lambda\phi) \tag{3.8}$$

can be used to represent a medium with sharply differentiated regions of permeability with the values $\kappa_0(1 \pm \alpha)$ by an appropriate choice of parameters. Clearly many other models can be constructed in the same spirit.

4. Perturbation theory for the effective permeability

King (1985), drawing on the methods of many-body theory, has shown how to calculate the effective permeability for a random medium from a perturbation series for $\bar{\mathcal{G}}(\boldsymbol{k})$. Similar methods have been used in discussions of turbulent diffusion (Phythian and Curtis 1978, Drummond *et al* 1984, 1986).

Here we will use the variable λ which appears in (3.2) as the expansion parameter for the perturbation series. Following standard reasoning (King 1985) we find

$$\bar{\mathcal{G}}(\boldsymbol{k}) = \frac{1}{\kappa_0 k^2 + \Sigma(\boldsymbol{k})} \tag{4.1}$$

where $c_0 = \kappa_0$ and $\Sigma(\boldsymbol{k})$ is a sum over terms each associated with a graph of the kind illustrated in figures 1–4, according to rules set out below.

Figure 1. One-loop contributions to the full Green function.

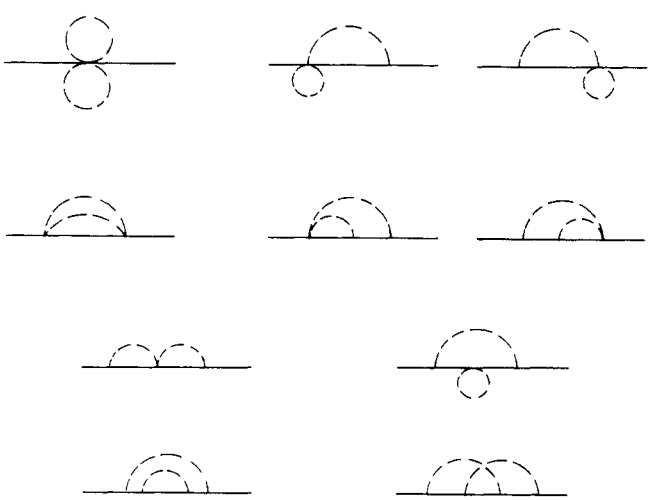

Figure 2. Two-loop contributions to the full Green function.

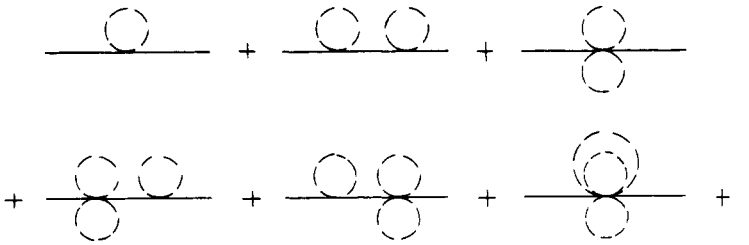

Figure 3. Bubble decorations which lead to the redefinition of the free Green function by means of the resummation described in (5.1) and (5.2).

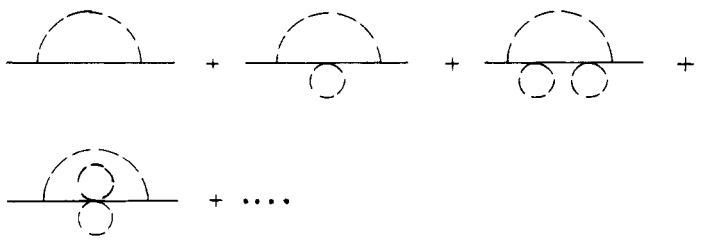

Figure 4. Bubble decorations on an internal line.

As we will see, each term in the series for $\Sigma(\boldsymbol{k})$ is $O(k^2)$ as $\boldsymbol{k} \to 0$. Hence

$$\sum(\boldsymbol{k}) = \sigma k^2 \qquad \boldsymbol{k} \to 0 \tag{4.2}$$

with the result that

$$\bar{\mathcal{G}}(\boldsymbol{k}) = \frac{1}{(\kappa_0 + \sigma)k^2} \qquad \boldsymbol{k} \to 0. \tag{4.3}$$

It follows immediately (see (2.11)) that the effective permeability is

$$\kappa_e = \kappa_0 + \sigma. \tag{4.4}$$

The graphical rules for the terms in the perturbation series are as follows.

(i) Associated with a line

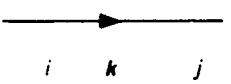

is a factor

$$-\frac{k_i k_j}{\kappa_0 k^2}.$$

(ii) Associated with a broken line

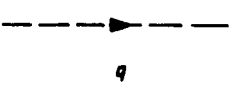

is a factor

$$\bar{\Delta}(\boldsymbol{q}).$$

(iii) Associated with a vertex with n-broken lines

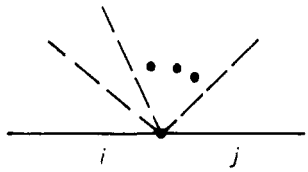

is a factor

$$\delta_{ij} c_n \lambda^n.$$

(iv) Momentum is conserved at each vertex.

(v) Each loop momentum $\boldsymbol{q}$ is integrated with a weight

$$\int \frac{\mathrm{d}^3 q}{(2\pi)^3}.$$

(vi) Internal cartesian suffixes are contracted in a natural way; the two external suffices are each contracted with the external wavevector.

(vii) The contribution of each graph is also divided by an appropriate symmetry factor.

The simplest contributions to $\Sigma(\boldsymbol{k})$ correspond to figure 1(a). We find, on applying the above rules, that

$$\sum^{(1a)}(\boldsymbol{k}) = \tfrac{1}{2} c_2 \lambda^2 k_i \int \frac{\mathrm{d}^3 q}{(2\pi)^3} \bar{\Delta}(q) \delta_{ij} k_j \tag{4.5}$$

i.e.

$$\sum^{(1a)}(\boldsymbol{k}) = \tfrac{1}{2} c_2 \lambda^2 k^2. \tag{4.6}$$

From figure 1(b) we obtain

$$\sum^{(1b)}(\boldsymbol{k}) = c_1^2 \lambda^2 k_i \int \frac{\mathrm{d}^3 q}{(2\pi)^3} \bar{\Delta}(q) \left(-\frac{(k-q)_i (k-q)_j}{\kappa_0 (k-q)^2} \right) k_j. \tag{4.7}$$

When $\boldsymbol{k}$ is small this yields

$$\sum^{(1b)}(\boldsymbol{k}) = -\frac{1}{3} \frac{c_1^2}{\kappa_0} \lambda^2. \tag{4.8}$$

The contributions of $\mathrm{O}(\lambda^4)$ are associated with the diagrams of figure 2. The final result then to $\mathrm{O}(\lambda^4)$ is

$$\kappa_e = \kappa_0 + \lambda^2 \left(\tfrac{1}{2} c_2 - \frac{1}{3} \frac{1}{\kappa_0} c_1^2 \right) + \lambda^4 \left(\tfrac{1}{8} c_4 - \frac{1}{\kappa_0} (\tfrac{1}{3} c_1 c_3 + \tfrac{1}{6} c_2^2) + \frac{1}{\kappa_0^2} c_1^2 c_2 (\tfrac{5}{18} + \tfrac{2}{3} I) - \frac{1}{3} \frac{1}{\kappa_0^3} c_1^4 (I + J) \right) \tag{4.9}$$

where

$$I = \frac{1}{8\pi^4} \int \mathrm{d}p \, \mathrm{d}q \, \bar{\Delta}(p) \bar{\Delta}(q) p^2 \left(\frac{3}{2} q^2 - \frac{1}{2} p^2 + \frac{(q^2 - p^2)^2}{4pq} \ln \left| \frac{p+q}{p-q} \right| \right) \tag{4.10}$$

and

$$J = \frac{1}{8\pi^4} \int \mathrm{d}p \, \mathrm{d}q \, \bar{\Delta}(p) \bar{\Delta}(q) \left[\tfrac{1}{3} p^2 q^2 - \tfrac{1}{4} (q^2 - p^2)^2 \left(1 - \frac{q^2 - p^2}{2pq} \ln \left| \frac{p+q}{p-q} \right| \right) \right]. \tag{4.11}$$

These integrals are readily evaluated by numerical integration for specific choices of correlation function $\bar{\Delta}(p)$.

5. Resummation and self-consistent perturbation theory

There is a natural resummation associated with the diagrams of figure 3 which make up a series with $\Sigma^{(1a)}$ as its first term. The whole series yields a contribution to σ of the form

$$\sigma = c_2\left(\frac{\lambda^2}{2}\right) + \frac{1}{2}c_4\left(\frac{\lambda^2}{2}\right)^2 + \frac{1}{3!}c_6\left(\frac{\lambda^2}{2}\right)^3 + \ldots . \tag{5.1}$$

The sum of this series is $\kappa_m - \kappa_0$ leading to the result

$$\kappa_0 + \sigma = \kappa_m . \tag{5.2}$$

When all these terms are included the lowest approximation to $\bar{\mathcal{G}}(\boldsymbol{k})$ is changed from $1/\kappa_0 k^2$ to $1/\kappa_m k^2$, i.e. κ_0 has been replaced by κ_m. A similar replacement occurs on every *internal* line if we add up all the bubble decorations it carries as indicated in figure 4. It follows that we can change the rules set out in § 4 by replacing κ_0 with κ_m provided we omit all bubble decorations to straight lines.

The result for the effective diffusivity can now be expressed as

$$\kappa_e = \kappa_m - \tfrac{1}{3}\lambda^2\frac{1}{\kappa_m}c_1^2 + \lambda^4\left(-\frac{1}{\kappa_m}(\tfrac{1}{3}c_1c_3 + \tfrac{1}{6}c_2^2) + \frac{1}{\kappa_m^2}c_1^2c_2(\tfrac{1}{9}+\tfrac{2}{3}I) - \frac{1}{3}\frac{1}{\kappa_m^3}c_1^4(I+J)\right). \tag{5.3}$$

The main point of this resummation is that it is better to perturb about the mean permeability κ_m, which has a direct physical significance, rather than the original parameter κ_0. We now argue that it is even better to perturb about the exact result. This means that in principle the lowest approximation to $\mathcal{G}(\boldsymbol{x}-\boldsymbol{x}')$ will have the exact long distance behaviour. The resulting equations constitute a self-consistent perturbation series as advocated by Phythian and Curtis (1978) and used by us in another context (Drummond *et al* 1984).

To derive the self-consistent series we re-express κ_m in the form

$$\kappa_m = \kappa_e - \eta_2 - \eta_4 - \ldots \tag{5.4}$$

where η_2 and η_4 are terms of $O(\lambda^2)$ and $O(\lambda^4)$ respectively. We then substitute this series for κ_m into (5.3) and demand that the equation remain consistent order by order in λ. The result to $O(\lambda^4)$ is

$$\eta_2 = -\frac{1}{3}\lambda^2\frac{1}{\kappa_e}c_1^2 \tag{5.5}$$

$$\eta_4 = \lambda^4\left[-\frac{1}{\kappa_e}\left(\tfrac{1}{3}c_1c_3 + \tfrac{1}{6}c_2^2 + \frac{1}{\kappa_e^2}c_1^2c_2(\tfrac{1}{9}+\tfrac{2}{3}I) + \frac{1}{\kappa_e^4}c_1^4(\tfrac{1}{9}-\tfrac{1}{3}(I+J))\right)\right]. \tag{5.6}$$

The self-consistent value of κ_m is obtained to $O(\lambda^4)$ by solving numerically the equation

$$\kappa_e = \kappa_m + \eta_2 + \eta_4 \tag{5.7}$$

where we regard η_2 and η_4 as those functions of κ_e given in (5.5) and (5.6).

6. Numerical simulation

As indicated in § 2, our numerical simulation of the effective permeability is based on the diffusion equation (2.5). There are two important aspects of this simulation. First, we need a method for constructing realisations of the Gaussian random field $\phi(\boldsymbol{x})$ from which the permeability field is constructed and, second, we need an effective algorithm for integrating the stochastic differential equation which corresponds to (2.5).

The Gaussian random field is constructed by a method which is a simplification of one introduced by Kraichnan (1976) and used by us (Drummond *et al* 1984, 1986) to construct turbulent velocity fields. We set

$$\phi(\boldsymbol{x}) = \left(\frac{2}{N}\right)^{1/2} \sum_{n=1}^{N} \cos(\boldsymbol{k}_n \cdot \boldsymbol{x} + \varepsilon_n) \tag{6.1}$$

where $\{\varepsilon_n\}$ and $\{\boldsymbol{k}_n\}$ are independently distributed random variables. Each phase, ε_n, is distributed uniformly over the whole angular range. If $P(\boldsymbol{k})$ is the probability distribution function for each $\boldsymbol{k}_n$, then it is easy to see that

$$\Delta(\boldsymbol{x}-\boldsymbol{y}) = \langle \phi(\boldsymbol{x})\phi(\boldsymbol{y})\rangle = \int \mathrm{d}^3\boldsymbol{k}\, P(\boldsymbol{k}) \cos[\boldsymbol{k}\cdot(\boldsymbol{x}-\boldsymbol{y})] \tag{6.2}$$

so that if $P(\boldsymbol{k})$ is an even function of $\boldsymbol{k}$ (which we assume) then it is essentially the Fourier transform of $\Delta(\boldsymbol{x}-\boldsymbol{y})$. We do not at this stage have any prejudice as to which forms for $P(\boldsymbol{k})$ are the most realistic. We choose

$$P(\boldsymbol{k}) = \frac{1}{(2\pi)^{3/2} k_0^3} \exp(-\tfrac{1}{2}k^2/k_0^2) \tag{6.3}$$

as a simple easily implemented form with a characteristic length scale k_0^{-1}. The Gaussian nature of the statistics of $\phi(\boldsymbol{x})$ is guaranteed by choosing N sufficiently large. We work with $N = 64$, which has proved to be a sufficiently large number.

In a recent paper (Drummond *et al* 1986) we studied numerical methods for integrating the stochastic differential equation corresponding to (2.5), where now we interpret $p(\boldsymbol{x}, \tau)$ as a probability distribution at 'time' τ for a particle located at position $\boldsymbol{x}$. The simplest discrete time-step form of the integration procedure is

$$\Delta\boldsymbol{x} = \nabla\kappa(\boldsymbol{x})\Delta\tau + (2\kappa(\boldsymbol{x})\Delta\tau)^{1/2}\boldsymbol{\eta} \tag{6.4}$$

where $\Delta\tau$ is the 'time step' and $\boldsymbol{\eta}$ is a vector whose components are independent Gaussian random variables with zero mean and unit variance. When implemented this algorithm yields a probability distribution which evolves with an error $O(\Delta\tau)$. We have found it better to use a higher-order method with errors which are $O(\Delta\tau^2)$. The algorithm for the step from $\boldsymbol{x} \to \boldsymbol{x}+\Delta\boldsymbol{x}$ has the form

$$\Delta\boldsymbol{x} = \nabla\kappa(\boldsymbol{y}_1)\Delta\tau + (\Delta\tau)^{1/2}\{(\kappa(\boldsymbol{x}))^{1/2}\boldsymbol{\eta} + [\beta(\kappa(\boldsymbol{y}_2))^{1/2} + \gamma(\kappa(\boldsymbol{y}_3))^{1/2}]\boldsymbol{\zeta}\} \tag{6.5}$$

where $\boldsymbol{\eta}$ and $\boldsymbol{\zeta}$ are independent Gaussian random vectors with zero mean and unit variance for each component. The parameters are

$$\begin{aligned} \beta &= \tfrac{1}{2}(\sqrt{2}+1) \\ \gamma &= -\tfrac{1}{2}(\sqrt{2}-1) \end{aligned} \tag{6.6}$$

and the intermediate points are given by

$$\begin{aligned} y_1 &= x + \tfrac{1}{2}\nabla\kappa(x)\Delta\tau + (\kappa(x)\Delta\tau)^{1/2}\eta \\ y_2 &= x + \tfrac{1}{2}\nabla\kappa(x)\Delta\tau + (2\kappa(x)\Delta\tau)^{1/2}\eta \\ y_3 &= x + \tfrac{1}{2}\nabla\kappa(x)\Delta\tau - (2\kappa(x)\Delta\tau)^{1/2}\eta. \end{aligned} \tag{6.7}$$

For each realisation of $\kappa(x)$, we introduce a particle at the origin at $\tau = 0$ and advance its position according to the above algorithm, measuring x^2 as it develops in 'time'. For large τ the mean of x^2, averaged over the particles and realisations of $\kappa(x)$, is linear in τ. The asymptotic slope is $6\kappa_e$.

An important check on the accuracy of the algorithm is that it correctly reproduces the correct result for the small τ behaviour of the probability distribution. For the mean square displacement we have

$$\langle x^2\rangle_\tau = \int \mathrm{d}^3x \, \langle x^2 \, \mathrm{e}^{\tau H}\delta(x)\rangle \tag{6.8}$$

where the angle brackets on the right indicate the average over the ϕ ensemble and

$$H = \partial_i\kappa(x)\partial_i. \tag{6.9}$$

After expanding the exponential and using the Hermiticity of the operator H we find

$$\langle x^2\rangle_\tau = \sum_{n=1}^{\infty} \frac{\tau^n}{n!}\langle H^n x^2\rangle|_{x=0}. \tag{6.10}$$

An evaluation of the first three terms yields

$$\langle x^2\rangle_\tau = 6\langle\kappa\rangle\tau + \langle\kappa\kappa_{ii}\rangle\tau^2 + \tfrac{1}{3}\langle\kappa\kappa_{ij}\kappa_{ij}\rangle\tau^3 + \ldots. \tag{6.11}$$

7. Results

We performed the numerical simulation for two different models: the polynomial model

$$\kappa\langle x\rangle = \kappa(1 + c\lambda\phi(x) + \tfrac{1}{2}\lambda^2\phi^2(x)) \tag{7.1}$$

and the log-normal model

$$\kappa(x) = \exp(\lambda\phi(x)). \tag{7.2}$$

Equation (6.11) implies that, for short 'times',

$$\langle x^2\rangle = 6(1 + \tfrac{1}{2}\lambda^2)\tau - 3\lambda^2(c^2 + \lambda^2)\tau^2 + \lambda^2[5c^2 + (10 + \tfrac{31}{2}c^2)\lambda^2 + 13\lambda^4]\tau^3 + \ldots \tag{7.3}$$

for the polynomial model and, for the log-normal model,

$$\langle x^2\rangle = 6\kappa_m\tau - 3\kappa_m^2\lambda^2\tau^2 + \kappa_m^3\lambda^2(5 + 8\lambda^2)\tau^3 + \ldots \tag{7.4}$$

where $\kappa_m = \exp(\frac{1}{2}\lambda^2)$. In both cases our algorithm gave results for small τ consistent with these formulae. We can be reasonably confident, therefore, of its accuracy.

At large τ, $\langle x^2\rangle$ increases linearly with a slope $6\kappa_e$. This allows us to obtain the effective permeability from the simulation. The comparison between our results and the predictions of self-consistent perturbation theory with $\kappa_0 = k_0 = 1$ are exhibited in figures 5 and 6 for the polynomial model and figure 7 for the log-normal model. When $k_0 = 1$, I and J have the values

$$I = 0.5708 \qquad J = 0.2275. \tag{7.5}$$

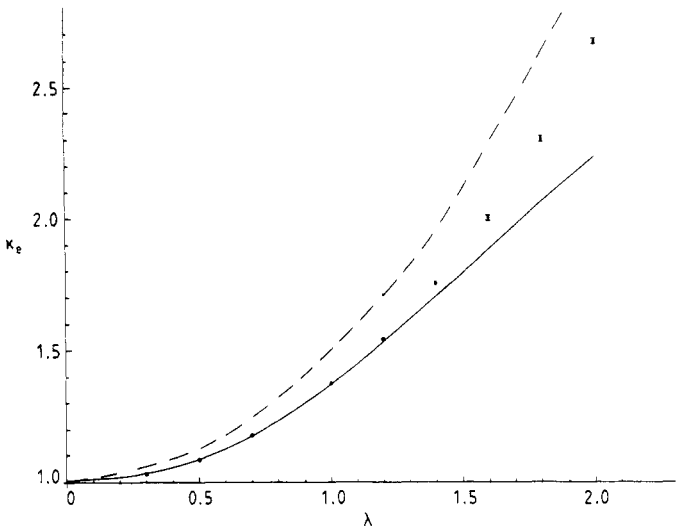

Figure 5. Effective permeability κ_e in the polynomial model, plotted against λ for $c = 0.7$. The full curve shows the results of self-consistent perturbation theory. The broken curve shows the mean permeability.

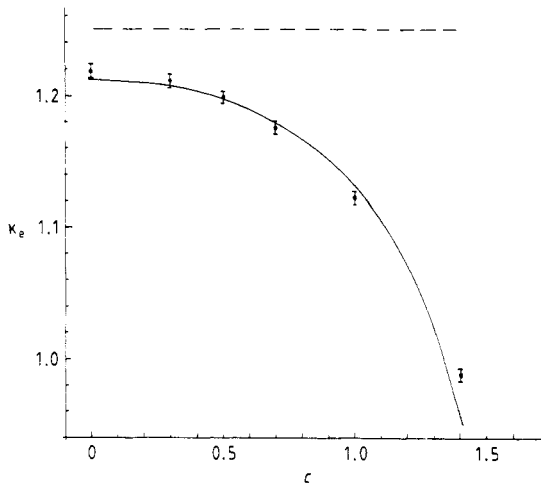

Figure 6. Effective permeability κ_e in the polynomial model, plotted against c, for $\lambda = 0.7$. The full curve shows the results of self-consistent perturbation theory. The broken line shows the mean permeability.

In both cases the simulation agrees with perturbation theory for a resonable range of parameters. In particular the inequality with which perturbation theory is consistent (King 1985)

$$\kappa_e < \kappa_m \tag{7.6}$$

clearly holds for both models.

The discrepancy between simulation and perturbation theory which develops in both models for large values of λ (figures 5 and 7) is no more than one should expect since for $\lambda = 1$ the $O(\lambda^4)$ terms in the perturbation expansion are comparable in size

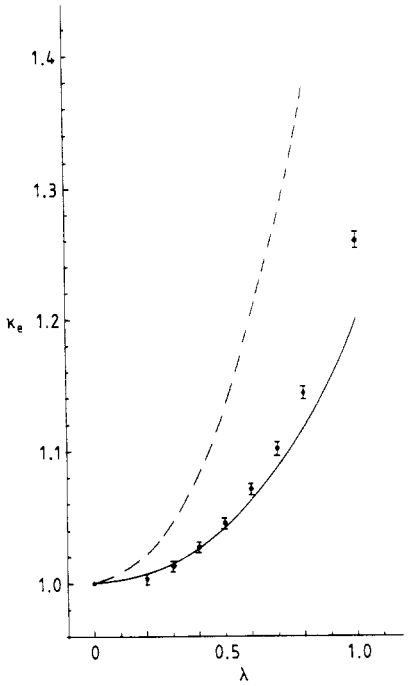

Figure 7. The effective permeability κ_e for the log-normal model, plotted against λ. The full curve shows the results of self-consistent perturbation theory. The broken curve shows the mean permeability.

to the discrepancy. An interesting feature of the results for the polynomial model is the discrepancy which appears as c passes through 1 and approaches 1.4. We note that the physical requirement that $\kappa(x) \geq 0$ implies the constraint $c \leq \sqrt{2}$. Since perturbation theory shows no particular features when c breaks this bound, it is not very surprising that this discrepancy shows up. On the contrary it is remarkable that perturbation theory continues to give such a reasonable account of the effective permeability for c so near its upper bound. A partial explanation may lie in the fact that while setting $c = \sqrt{2}$ introduces regions of zero or very low permeability, these remain sparsely distributed for small λ. For $c = \sqrt{2}$ and large λ, these impermeable regions may become so dense as to introduce a percolation threshold in λ at which the effective permeability will vanish.

Our main conclusions are that, on the one hand, perturbation theory methods drawn from solid state physics are useful in effective permeability calculations and, on the other hand, the diffusion simulation techniques we have developed are also practical means of computing effective parameters. They may be expected to be more widely applicable than perturbation theory. All that they require is a computable model of the inhomogeneous medium.

Our simulations were performed on the ICL DAP at Queen Mary College, London. Our second-order algorithm used a time step $\Delta\tau$ in the range 0.05–0.1 corresponding roughly to two or three compound steps or 4–6 primitive steps per correlation length in any given direction. The algorithm is sufficiently good for our results to be insensitive to changes in $\Delta\tau$ over the range indicated above. The statistical errors we quote are the result of following 1.5×10^5 particle paths.

We can envisage two immediate extensions of our work. First it is interesting to simulate the effective permeability in models other than the two considered in this paper. In particular we would like to investigate the percolation effects that might be observable in a medium divided in varying proportions between permeable and impermeable material. Second we wish to extend the computation to pressure fluctuations and their relationship with the permeability structure of different models.

Finally we would like to emphasise the generality of our simulation technique and its applicability to a much wider class of models of heterogeneous media than was considered in this paper.

References

Dullien F A L 1979 *Porous Media. Transport and Pore Structure* (New York: Academic)
Drummond I T, Duane S and Horgan R R 1984 *J. Fluid Mech.* **138** 75
Drummond I T, Hoch A and Horgan R R 1986 *J. Phys. A: Math. Gen.* **19** 3871
Drummond I T and Horgan R R 1986 *J. Fluid Mech.* **163** 425
King P R 1985 *Preprint* BP Research Centre, Sunbury-on-Thames, UK
Kraichnan R H 1976 *J. Fluid Mech.* **77** 753
Phythian R and Curtis W D 1978 *J. Fluid Mech.* **89** 241
Scheidegger A E 1974 *The Physics of Flow Through Porous Media* (Toronto: University of Toronto Press)